Lawrence Berkeley National Laboratory

Title
APPLICATION OF A LOW ENERGY X-RAY SPECTROMETER TO ANALYSES OF SUSPENEED AIR PARTICULATE MATTER

Permalink
https://escholarship.org/uc/item/9k88p78w

Author
Giauque, R.D.

Publication Date
1975-09-01

APPLICATION OF A LOW ENERGY X-RAY SPECTROMETER TO ANALYSES OF SUSPENDED AIR PARTICULATE MATTER

R. D. Giauque, R. B. Garrett, L. Y. Goda,
J. M. Jaklevic, and D. F. Malone

September 12, 1975

DISCLAIMER

LBL 4402

APPLICATION OF A LOW ENERGY X-RAY SPECTROMETER TO ANALYSES OF

SUSPENDED AIR PARTICULATE MATTER.*

R. D. Giauque, R. B. Garrett, L. Y. Goda,

J. M. Jaklevic, and D. F. Malone

Lawrence Berkeley Laboratory

Berkeley, California 94720

ABSTRACT

A semiconductor detector x-ray spectrometer has been constructed
for the analysis of elements in air particulate specimens. The exci-
tation radiation is provided, either directly or indirectly, using a
low power (40 watts) Ag anode x-ray tube. Less than 100 ng for most
of the elements in the range Mg → Zr, Pb are easily detected within
two 1-minute counting intervals. A calibration technique for light
element analysis and an experimental method which compensates for
particle size effects will be discussed.

INTRODUCTION

The analytical technique of x-ray induced x-ray fluorescence
analysis (XRFA) lends itself to the simultaneous determination of a
broad range of elements in environmental specimens. Both energy dis-
persive and wavelength dispersive spectrometers are presently employ-
ed at various laboratories for analyses of air particulate specimens
collected on thin substrates (1-8). For many elemental analyses, air
particulate specimens are ideal for XRFA methods in that they are "in-
finitely" thin specimens and the concentration of an element is di-

rectly proportional to the intensity of one of its x-ray lines. Typically, either photons produced by an x-ray tube or particles (protons or alpha) provided by an accelerator are employed for excitation in analyses. Higher sensitivities have been reported using x-ray induced XRFA methods for the determination of elements of atomic number 20 (Ca) and higher, while particle induced XRFA methods have obtained higher sensitivities for lower atomic number elements (9). However, since the characteristic x-rays of low atomic number elements undergo significant absorption within the sample, additional considerations must be made when determining their concentration, including corrections for particle size effects, heavy particulate loadings, and for absorption in the filter media due to the penetration of the particles into the substrate. Present methods for particle size corrections have been based on assumptions of the particle compositions and of the particle size distribution for non-size segregated air particulate specimens (10, 11). Models for deriving corrections for absorption effects due to particle penetration in the filter media have also been suggested (7, 11).

We have developed a technique for performing energy dispersive analysis of light elements in air particulate samples. An x-ray spectrometer especially designed for the detection of low energy x-rays has been used to measure the concentration of both high and low (down to Mg) atomic number elements. A technique to compensate for particle size effects has been applied to the analysis. This technique makes use of multiple energies of x-ray excitation which act as variable depth probes when determining the concentration of the light elements. Comparison of our results with neutron activation analyses (NAA) demonstrates the good agreement achieved by our calibration and correction procedures.

DISCUSSION OF METHOD

The XRFA method involves the interaction of photons from an x-ray source with specimen atoms to create inner atomic shell vacancies; subsequent atomic transitions fill the vacancies and a fraction of these give rise to the emission of characteristic x-rays which are detected and utilized for analysis. Detailed descriptions of the x-ray processes are reviewed in the literature (12-14).

The energy of the excitation radiation selected for analysis heavily influences sensitivities attainable. Table I lists x-ray

photoelectric cross-sections of selected elements for AgLα (3.0 keV), NiKα (7.5 keV), and MoKα (17.4 keV) x-rays (15). As shown, AgLα x-rays are over 100 times more efficient than MoKα x-rays for producing photoelectric interactions with the elements Al → Cl. Likewise, NiKα x-rays are approximately 10 times more efficient than MoKα x-rays for producing photoelectric interactions with the elements Al → Fe. Consequently, excitation radiations of more than one energy are utilized for the analysis of a broad range of elements.

Table 1. Photoelectric Cross Sections

Excitation radiation	AgLα 3.0 KeV	NiKα 7.5 KeV	MoKα 17.4 KeV
Element			
Al	810 cm^2/gm	62 cm^2/gm	4.9 cm^2/gm
Si	990	80	6.4
S	1360	113	9.4
Cl	1430	132	11
K		179	16
Ca		207	19
Fe		363	37
Cu			49
Br			74

INSTRUMENTATION

A number of methods for generating variable energies of excitation radiation have been used in previous x-ray systems, including multiple x-ray anodes (16) and secondary fluorescence targets (1, 17). As an alternative approach we have designed a spectrometer which permits the utilization of both direct and indirect excitation radiation, by the use of transmission filters and secondary targets respectively as shown in Figures 1 and 2. The cryostat design allows the excitation radiation to pass through the vacuum cryostat, permitting very large solid angles and minimum x-ray attenuation. An air path
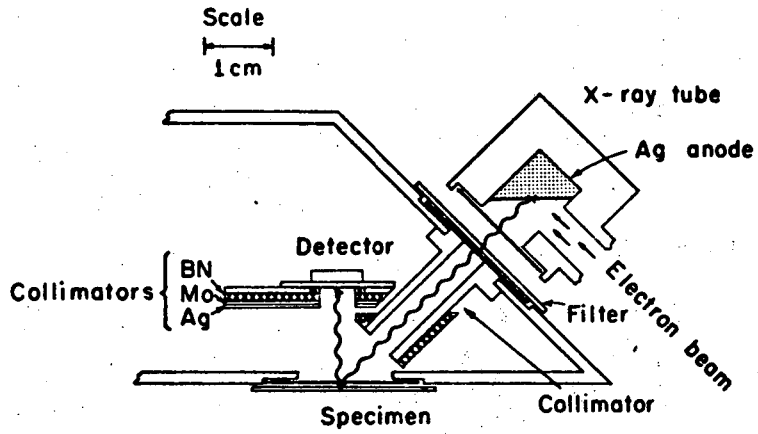
Figure 1.   X-ray spectrometer in direct excitation
            mode.
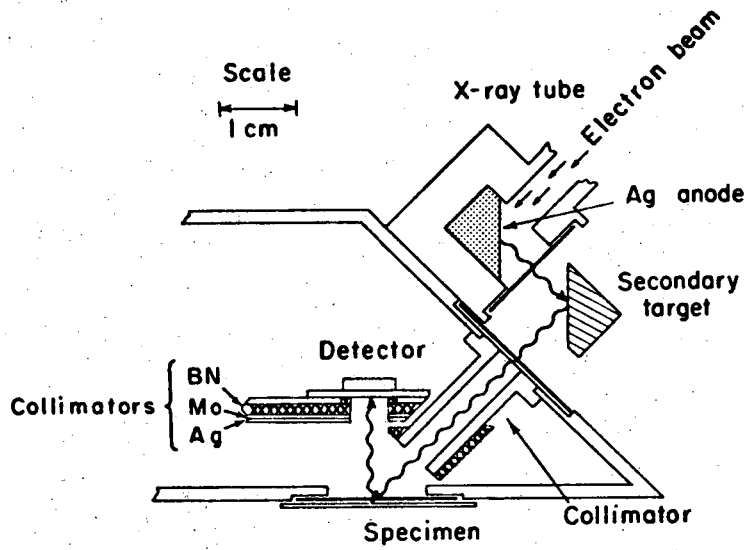
Figure 2.   Spectrometer in secondary excitation
            mode.

length of only 1.5 mm exists between the specimen and the detector
window (0.002 cm Be). This enhances sensitivity for low atomic num-
ber elements (Z < 20, Ca) which have x-ray energies <4 keV. Also,
with this system, small total specimen areas, 1 cm^2, are required. In
the direct excitation mode, high excitation efficiencies are achieved,
(1) for low Z elements using AgL x-rays, and (2) for high Z elements
using AgK x-rays. Transmission Ag filters are inserted to modify the
x-ray tube output. Typical count rates are 5-10 K counts/sec using a
low power x-ray tube. The detector, which has an effective area of
40 mm^2, has been collimated to an area of approximately 30 mm^2. This
modification enhances sensitivities attainable when AgK x-rays are
used for analyses (18, 19). This minimizes the fraction of the high
energy radiation detected near the periphery of the sensitive region
of the detector, which otherwise would substantially increase the re-
sulting spectrum background in the region of interest.


ANALYTICAL METHOD

Air particulate matter collected on filters (membrane type) of im-
pactor media can be treated as thin specimens with negligible absorp-
tion effects for many elemental analyses. We define a thin specimen
as a mass m(g/cm^2) <0.02/μ, where μ(cm^2/g) is the sum of the specimen
mass absorption coefficients for the excitation and fluorescent radia-
tions. Such a mass would experience less than 1% attenuation effect.
In these cases, the concentration of an element is directly proportional
to the intensity (I_j) of one of its K or L x-ray lines and may be ex-
pressed

$$I_j = K_j m_j \qquad (1)$$

where K_j is a sensitivity factor for the element j.

Particle Size Effects

When analyzing for lower atomic number elements such as Al, Si,
S, Cl, K, and Ca, appropriate considerations must be undertaken to com-
pensate for particle size effects (mainly absorption effects). The
characteristic x-rays from these elements are low in energy, <4 keV,
and the thin specimen criteria is often not valid. These elements are
frequently present at above or near the level of 1 μg/m^3 of air in ur-
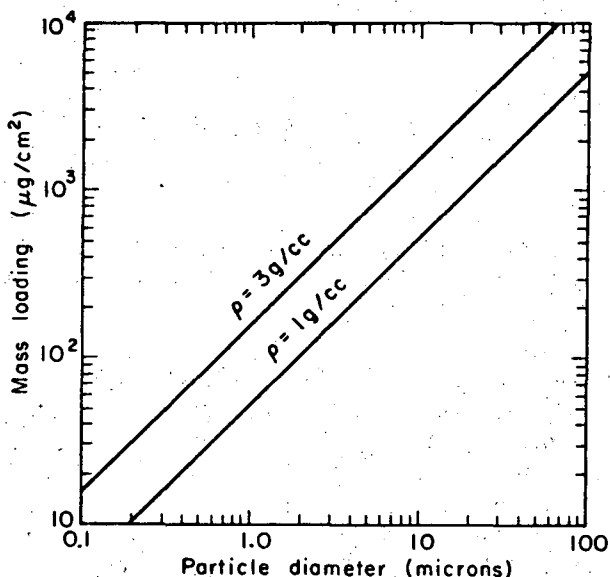
XBL757-3541

Figure 3. Plot of maximum mass loading permissible
for the monolayer criteria.

ban aerosols. The elements Al, Si, K, and Ca are principally in parti-
cles > 1μ in diameter, whereas S is usually associated with smaller
particles.

Typical mass loadings collected for XRFA are in the 50-200 μg/cm^2
range. In the approach we use to compensate for particle size effects,
we assume that particles several microns and larger are collected in
the form of a monolayer. Figure 3 shows plots of the maximum mass
loadings permissible for the monolayer criteria if the particles were
arranged as hexagonal close-packed spheres. In reality, somewhat lower
mass loadings are required due to the random distribution of the parti-
cles. Monolayer conditions can easily exist for mass loadings up to
150 μg/cm^2 for particles of aerodynamic diameters of 4μ and greater.

Although particulate matter is a heterogeneous mixture in which
the particle sizes, shapes, and composition vary, the characteristic
x-ray intensity (I_c) from a given element in a particle of average mass

thickness ($\overline{m}$), g/cm^2, may be approximated as

$$I_c = I_{thin}[1-exp-(\mu_e+\mu_f)\overline{m}]/(\mu_e+\mu_f)\overline{m} \tag{2}$$

where I_{thin} = the characteristic x-ray line intensity from an equal amount of the particle distributed "infinitely" thin (no absorption effects), μ_e and μ_f are the total mass absorption coefficients (cm^2/g) of the particle for the excitation and the fluorescent radiations, respectively.

If two different energies of excitation radiation are applied separately for analyses, the ratio of the two mass concentrations determined (uncorrected for absorption effects) may be described

$$m_2/m_1 = [1-exp-r(\mu_{e_1}+\mu_f)\overline{m}]/r[1-exp-(\mu_{e_1}+\mu_f)\overline{m}] \tag{3}$$

where

$$r = (\mu_{e_2}+\mu_f)/(\mu_{e_1}+\mu_f)$$

and μ_{e_1} and μ_{e_2} are the total mass absorption coefficients of the particle for the two excitation radiation energies. For a specific pair of excitation energies the value of "r" can be relatively independent of the particle composition. The ratio m_2/m_1 then becomes a function of the particle size absorption correction term in equation (2). Thus, it is possible to use the ratio m_2/m_1 to determine the correction for particle size effects.

Large particles in the atmospheric aerosols are principally from a mechanical process such as wind blown soil dust and usually consist of certain minerals such as kaolinite, anorthite, microline, and albite (20). For specific excitation radiations such as ZrL, AgL, or NiK x-rays, the total mass absorption coefficients of these minerals are similar for Si and Al. Table II shows the ratio of the total mass absorption coefficients ("r" in equation 3) for given pairs of these radiations. For this choice of minerals the value of "r" is relatively constant. Figure 4 shows curves for "r" values which could be used for Si or Al mass concentration determinations with ZrL and AgL excitation radiations. These curves are plotted with the ratio of the mass con-

Table II. Total Mass Absorption Coefficient Ratios

Excitation radiations	ZrL/AgL		NiK/AgL	
Element of Interest	Al	Si	Al	Si
Mineral				
Kaolinite $Al_2(Si_2O_3)(OH)_4$	1.51	1.49	0.77	0.78
Anorthite $CaAl_2Si_2O_8$	1.53	1.49	0.77	0.79
Microline $KAlSi_3O_8$	1.56	1.60	0.77	0.74
Albite $NaAlSi_3O_8$	1.53	1.58	0.75	0.72

$$\frac{m_2}{m_1}$$

$r = 1.50$

$r = 1.55$

$r = 1.60$

$$(\mu_{e_1} + \mu_f)\overline{m} \,/\, [1-exp-(\mu_{e_1} + \mu_f)\overline{m}]$$
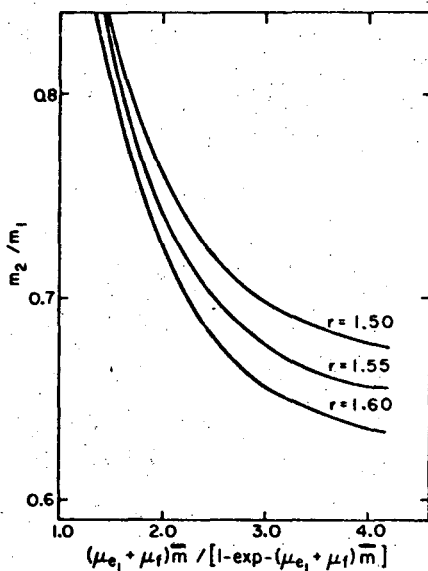
XBL747-3788A

Figure 4. Absorption correction curves for Si and Al mass concentration determination.

centrations (uncorrected for absorption effects) versus the absorption correction term to be applied to compensate for absorption effects when analyzing with AgL x-rays. The utility of our method requires that the value of "r" chosen be fairly well known and that the particles not be of infinite thickness (absorption correction term <4.0).

The mass concentration from a total of n particles may then be expressed

$$m = \sum_{i=1}^{n} m_i [(\mu_e + \mu_f)\bar{m}_i / (1 - \exp - (\mu_e + \mu_f)\bar{m}_i)] \tag{4}$$

This summation can be performed independent of the energy of the excitation radiation employed, presuming infinite thickness is not attained, $(\mu_e + \mu_f)\bar{m} < 4$, for the individual particles. The value for $(\mu_e + \mu_f)\bar{m}$ may be determined and, in turn, the value of m is ascertained. Although this procedure requires that a weighted average value for m be used, the net error in the result is small. This is due to the fact that the bulk of the mass concentration is usually within a relatively small range, since the total mass of a particle can vary as the cube of the particle diameter.

For our determinations with ZrL and AgL x-rays, we initially select an "r" value of 1.55. We make an additional analysis, using NiK x-rays for excitation, to verify that our results confirm this to be the correct value. If many particles of "infinite thickness" were present, verification could not be obtained. In such a case a minimum mass concentration would be reported.

The advantages of the semi-empirical method for particle size corrections derive from its relative lack of assumptions regarding the size distribution of the collected particles. Size distribution models have limited applicability in general usage, since meteorological conditions and sampling techniques can greatly change the results.

Evaluation of Filter Absorption Effects
Due to Penetration of Small Particles

Even though membrane type filters are often used to collect the aerosol specimens, a fraction of the fine particles which are smaller than the filter pores will penetrate into the filter medium. Filter absorption effects occur when the fine particles contain elements for

which low energy x-rays (<4 keV) are chosen for analyses. The fine par-
ticles usually arise from combustion processes, either directly or in-
directly. Both Dzubay and Bonner have assumed that the mass concentra-
tion decreases exponentially with penetration depth in the filter (7, 11).

To explore the degree of particle penetration in a 1.2μ cellulose
ester membrane filter, fresh combustion particles were collected in a
vehicular tunnel with dichotomous virtual impactors (22). One of the
specimens containing the small particulate fraction was examined with
a scanning electron microscope (SEM) by Dr. Thomas Hayes of L.B.L. Fig-
ure 5 is a graphical illustration of the particulate deposit collected
on the filter. The blank filter is composed of strands of globular bodies
and has pores approximately 5μ in diameter and 10μ deep. The mass loading
of this specimen was 60 μg/cm^2 and over 75% of the total aerosol mass
was in the 0.1 - 0.3μ range (23). The maximum penetration depth observed
was 10μ. This determination was made from a cross section of the speci-
men. Particulate S is usually present in the submicron size range and
can penetrate into the filter. Hypothetically, if the particulate S were

Pore diam ~5μm

Filter face

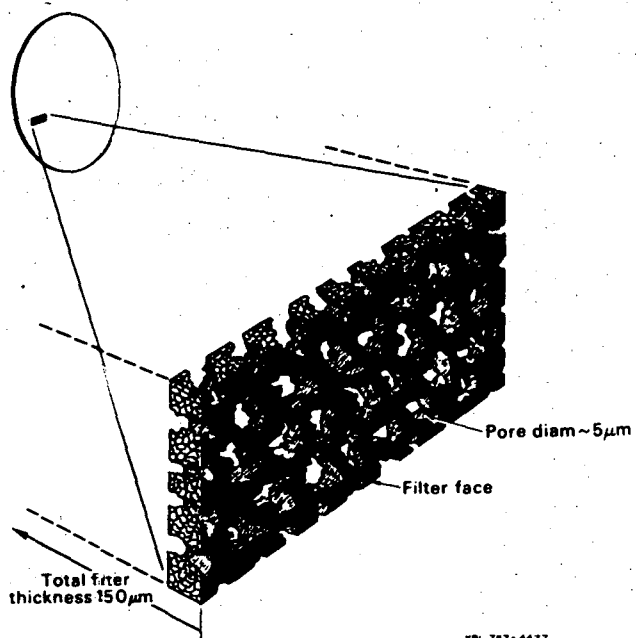Total filter
thickness 150μm

XBL 757-4477

Figure 5. Graphical illustration of particulate
deposit collected on cellulose ester
membrane filter.

deposited uniformly across the filter down to a 10μ depth as a homogene-
ous mix with the filter, the net absorption effect, when AgL x-rays are
used as the excitation radiation, would be approximately 7%. However,
the particles are collected principally on the surface of the filter and
since our detection system is parallel to the filter surface, shadowing
effects for the low-energy fluorescent x-rays are minimized. From these
facts we conclude that absorption effects for the S analysis due to parti-
cle penetration is minor and much less than 5% when 1.2μ cellulose ester
membrane filters are used. We have further substantiated our conclusions
by selecting three different excitation radiations, AgL, TiK, and NiK
x-rays, for analysis of S in aerosol specimens collected in Los Angeles.
(For the 45° excitation - specimen geometry, these excitation radiations
would act as probes into the filter.) The S results typically agreed to
within several percent. SEM photographs of the specimen collected in the
vehicular tunnel indicate that absorption effects due to conglomeration
of the small particles could be a more serious problem than absorption
effects due to penetration of the particles. For this problem we do not
have a solution.

Calibration Method

Ideally, one would like to have thin standards with negligible
absorption effects (<1%) for each of the elements in order to deter-
mine the sensitivity factor, K_j, in equation 1. However, this is not
practical since some elements are too volatile or reactive in their ele-
mental form (e.g., Cl, Br, I, Hg, K, Ca, Rb, Sr) or their compounds are
hydroscopic. Fortunately, the relative ability to excite and detect
x-rays can be calculated. As previously reported, this process is
straightforward when near monochromatic excitation radiation is employed
(21).

A thick pure Si disk is used to standardize the spectrometer for
the analyses of the lower Z elements since a truly thin uniform standard
with negligible absorption effects would be difficult to prepare. For
this paper, the mass of a thick element disk is defined

$$(\mu_e csc\phi_1 + \mu_f csc\phi_2)m_{thick} = 3.92$$

where ϕ_1 and ϕ_2 are the angles formed by the excitation and the fluores-
cent radiations with the disk surface. Since mass m_{thick} represents the
mass for which only 25% of the radiation (excitation x fluorescent) is
not attenuated, the mass of the disk for calibration purposes equals

$m_{thick}/4.0$. We have utilized this same procedure to standardize for Al and S and obtained agreements to within 5% of the calculated relative excitation-detection efficiency values normalized to Si. For these calculations corrections were applied to compensate for the detector dead layer (equivalent surface mass for which ionization events are not measured) and for absorption b_m the very thin Au layer on the surface of the detector. For this spectrometer these attenuation corrections for Mg → Ca K x-rays were in the range of 5 to 15%.

RESULTS

For the analyses of the lower Z elements in the direct excitation mode, the x-ray tube is operated at 9 KV and 200 μamps. A 0.00025 cm Ag filter is positioned externally to the x-ray tube to convert Bremstrahlung from the tube to AgL x-rays. A small amount of Bremstrahlung with a maximum intensity at 6 keV passes through the Ag filter and is used to analyze for the elements K and Ca. Figure 6 shows a spectrum obtained of an aerosol specimen collected on a cellulose ester substrate. The elemental values listed are, in $μg/cm^2$.
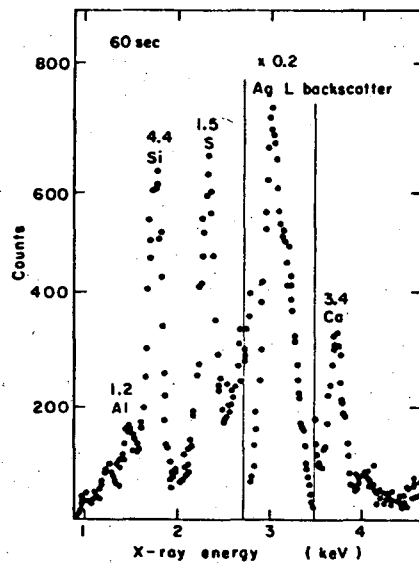

XBL757-3421

Figure 6. Spectrum of air particulate specimen.

Table III.   Theoretical Limits of Detection

Mode	Secondary Target			Direct	
	Zr	Ag	Ni	.00025 cm Ag Filter	.025cm V .007cm Ag filters
Element and Spectral line	ng/cm^2	ng/cm^2	ng/cm^2	ng/cm^2	ng/cm^2
MgKα	-	-	-	80	-
AlKα	250	400	1200	40	-
SiKα	160	190	440	20	-
SKα	-	110	190	12	-
ClKα	-	130	140	16	-
CaKα	-	-	50	28	-
FeKα	-	-	50	-	140
ZnKα	-	-	-	-	30
PbLα	-	-	-	-	50
BrKα	-	-	-	-	20

Table IV.   Analysis of Aerosol Specimens

No.	Method	Al	Ca	Br
1	XRF	$2.4+0.5$ $\mu g/cm^2$	$2.3+0.2$ $\mu g/cm^2$	$0.21+0.01$ $\mu g/cm^2$
	NAA	$2.3+0.1$	$3.1+0.4$	$0.19+0.01$
2	XRF	$9.0+2.7$	$6.2+0.3$	$0.21+0.01$
	NAA	$5.7+0.1$	$5.3+1.9$	$0.18+0.01$
3	XRF	$0.7+0.2$	$0.5+0.1$	$0.15+0.01$
	NAA	$1.1+0.1$	$0.8+0.3$	$0.11+0.01$
4	XRF	$0.3+0.2$	$0.3+0.1$	$0.15+0.01$
	NAA	$0.4+0.1$	$0.4+0.2$	$0.12+0.01$

For the analysis of higher Z elements the x-ray tube is operated at 37 KV and 600 μamps. A 0.007 cm Ag filter preceeded by a 0.025 cm V filter are employed. The V filter substantially reduces the Bremstrahlung transmitted between 6 and 14 keV and enhances sensitivities attainable for elements which have fluorescent x-rays in this range.

In the secondary excitation mode which is utilized for the particle size effect determinations, considerably lower sensitivities are attained due to a much lower overall geometrical factor. The x-ray tube is operated at 17 KV and 1,000 μamps with the Zr secondary target and at 22 KV and 1,000 μamps with the Ag and Ni secondary targets. Table III lists the sensitivities (3σ) attained in each of the direct and indirect excitation modes using 10 minute analysis times. The filter substrate used for these determinations was a cellulose ester membrane filter of mass 5 mg/cm^2. Typically, between 5 and 10 minute counting periods are necessary for each analysis using secondary targets for particle size effect determinations. The somewhat poor sensitivity for Fe in the direct excitation mode reflects the high background due to a small amount of Fe in the Be window through which both the excitation and fluorescent radiation pass.

Table IV lists a comparison of results acquired by x-ray fluorescence and neutron activation analyses of two-hour aerosol specimens collected during the California Aerosol Characterization Experiment in 1973. The neutron activation analyses were performed by R. Ragaini of the Lawrence Livermore Laboratory. Relatively good agreements were obtained by the two techniques for Al, Ca, and Br. The large uncertainty in the XRF Al value for specimen #2 reflects the uncertainty in the ascertained absorption correction factor which was 2.9. As shown in Figure 4, an uncertainty of 3% in the chosen "r" value could yield a 15 to 30% error in the result for such a large ascertained absorption correction factor. This factor corresponds to particles around 25μ (for unit density spheres).

We have applied our particle size correction techniques to the analysis of specimens collected from a number of regions and presumably representing a considerable variation in particle composition. These results have been in good agreement with NAA.

ACKNOWLEDGMENTS

-15-

REFERENCES

1. J.M. Jaklevic, F.S. Goulding, B.V. Jarrett, and J.D. Meng, "Application of X-Ray Fluorescence Techniques to Measure Elemental Composition of Particles In the Atmosphere", in R.K. Stevens and W.F. Herget, Editors, Analytical Methods Applied to Air Pollution Measurements, p. 123-146, Ann Arbor Science Publishers, Inc. (1974).

2. R.G. Flocchini, D.J. Shadoan, T.A. Cahill, R.A. Eldred, P.J. Feeney, and G. Wolfe, "Energy, Aerosols and Ion-Excited X-Ray Emissions", in W.L. Pickles, Editor, Advances in X-Ray Analysis, Vol. 18, p. 579-587, Plenum Press (1975).

3. R. Akselsson, C. Orsini, D.L. Meinert, T.B. Johansson, R.E. Van Grieken, H.C. Kaufmann, K.R. Chapman, J.W. Nelson, and J.W. Winchester, "Application of Proton Induced X-Ray Emission Analysis to the St. Louis Regional Air Pollution Study", Ref. 2, p. 588-597.

4. L.S. Birks, J.V. Gilfrich, and P.G. Burkhalter, "Development of X-Ray Fluorescence Spectroscopy for Elemental Analysis of Particulate Matter in the Atmosphere and in Source Emissions", Environmental Protection Agency Report, EPA-R2-72-063 (1972).

5. J.R. Rhodes, A.H. Pradzynski, C.B. Hunter, J.S. Payne, and J.L. Lindgren, "Energy Dispersive X-Ray Fluorescence Analysis of Air Particulates in Texas," Environmental Sci. Tech., 6 (10), p. 922-927 (1972).

6. T.G. Dzubay and R.K. Stevens, "Application of X-Ray Fluorescence to Particulate Measurements", Inst. Soc. Amer. JSP 6695, p. 211-216 (1973).

7. N.A. Bonner, F. Bazan, and D.C. Camp, "Elemental Analysis of Air Filter Samples Using X-Ray Fluorescence", Lawrence Livermore Laboratory Report, UCRL-51388, Livermore, Calif. (1973).

8. R.D. Giauque, L.Y. Goda, R.B. Garrett, "X-Ray Induced X-Ray Fluorescence Analysis of Suspended Air Particulate Matter", Lawrence Berkeley Laboratory Report LBL-2951, Berkeley, California (1974).

9. D.C. Camp, A.L. VanLehn, J.R. Rhodes, and A.H. Pradzynski, "Intercomparison of Trace Element Determinations in Simulated and Real Air Particulate Samples", X-Ray Spectrometry 4, p. 123-137 (1975).

10. J.R. Rhodes and C.B. Hunter, "Particle Size Effects in X-Ray Emission Analyses: Simplified Formulas for Certain Practical Cases", X-Ray Spectrometry 1, p. 113-117 (1972).

11. T.G. Dzubay and R.O. Nelson, "Self Absorption Corrections for X-Ray Fluorescence Analysis of Aerosols", Ref. 2, p. 619-631.

12. H.A. Liebhafsky, J.G. Pfeiffer, E.H. Winslow, and P.D. Zemany, X-Rays, Electrons, and Analytical Chemistry, Wiley-Interscience (1972).

13. R. Jenkins, An Introduction to X-Ray Spectrometry, Heyden (1974).

14. L.S. Birks, X-Ray Spectrochemical Analysis, Interscience Publishers (1969).

15. W.H. McMaster, N.K. Del Grande, J.H. Mallett, and J.H. Hubbell, "Compilation of X-Ray Cross Sections", Univ. of California, Lawrence Laboratory Report UCRL-50174, Section II, Revision I (1969), National Technical Information Service.

16. G.R. Dyer, D.A. Gedcke, and T.R. Harris, "Fluorescence Analysis Using an Si(Li) X-Ray Energy Analysis System with Low-Power X-Ray Tubes and Radioisotopes", in K.F.J. Heinrich, Editor, Advances in X-Ray Analysis, Vol. 15, p. 228-239, Plenum Press (1972).

17. D.E. Portor and R. Woldseth, "X-Ray Energy Spectrometry", Anal. Chem. 45, p. 604A-614A (1973).

18. F.S. Goulding, J.M. Jaklevic, B.V. Jarrett, and D.A. Landis, "Detector Background and Sensitivity of Semiconductor X-Ray Fluorescence Spectrometers", Ref. 16, p. 470-482.

19. R. Woldseth, X-Ray Energy Spectrometry, published by Kevex Corporation, Burlingame, Calif. (1973).

20. E.L. Kothny, California Department of Public Health, Berkeley, California, private communication, 1973.

21. R.D. Giauque, F.S. Goulding, J.M. Jaklevic, and R.H. Pehl, "Trace Element Determination with Semiconductor Detector X-Ray Spectrometers", Anal. Chem. 45, p. 671-681 (1973).

22. B.W. Loo, J.M. Jaklevic, and F.S. Goulding, "Dichotomous Virtual Impactors for Large-Scale Monitoring of Airborne Particulate Matter", Lawrence Berkeley Laboratory Report LBL-3854, Berkeley, Calif. (1975).

23. P. Bekowies, Lawrence Berkeley Laboratory, Berkeley, Calif., private communication, 1975.